

## Dansyl appended Cu<sup>II</sup>-complex based Nitroxyl (HNO) sensing with living cell application and DFT studies

Debjani Maiti,<sup>a</sup> Abu Saleh Musha Islam<sup>a</sup>, Ananya Dutta<sup>a</sup>, Mihir Sasmal<sup>a</sup>, Chandraday Prodhan,<sup>b</sup> and Mahammad Ali<sup>\*,a,c</sup>

<sup>a</sup>Department of Chemistry Jadavpur University, Kolkata 700 032, India; Fax: 91-33-2414-6223, E-mail: m\_ali2062@yahoo.com, mali@chemistry.jdvu.ac.in

<sup>c</sup>Vice-Chancellor, Aliah University, II-A/27, Action Area II, Newtown, Action Area II, Kolkata, West Bengal 700160,

### Supporting Information

No.	Content.	Figure.No.
1.	<sup>1</sup> H NMR spectrum of (L <sup>1</sup> ) in DMSO- <i>d</i> <sub>6</sub> .	<b>Fig.S1</b>
2	<sup>13</sup> C NMR spectrum of (L <sup>1</sup> ) in DMSO- <i>d</i> <sub>6</sub> .	<b>Fig. S2</b>
3.	Mass spectrum of spectrum of (L <sup>1</sup> ) in MeCN.	<b>Fig.S3</b>
4.	<sup>1</sup> H NMR spectrum of DQ <sub>468</sub> in DMSO- <i>d</i> <sub>6</sub> (300Mz).	<b>Fig. S4</b>
5.	<sup>13</sup> C NMR spectrum of DQ <sub>468</sub> in DMSO- <i>d</i> <sub>6</sub> .	<b>Fig. S5</b>
6.	Mass spectrum of DQ <sub>468</sub> in MeCN.	<b>Fig. S6</b>
7.	Ir spectrum of DQ <sub>468</sub> .	<b>Fig. S7</b>
8.	Solvent selectivity of Cu(II)-complex formation.	<b>Fig.S8</b>
9.	LOD of DQ <sub>468</sub> to Cu <sup>2+</sup>	<b>Fig.S9</b>
10.	Mass spectrum of [Cu <sup>II</sup> (DQ <sub>468</sub> )Cl].	<b>Fig. S10</b>
11.	Metal ion selectivity test of DQ <sub>468</sub>	<b>Fig. S11</b>
12.	Water variation on HNO induced reduction of Cu(II)-complex.	<b>Fig. S12</b>
13.	LOD of [Cu <sup>II</sup> (DQ <sub>468</sub> )Cl] to HNO.	<b>Fig. S13</b>
14.	Mass spectrum of [Cu(DQ <sub>468</sub> )Cl]+ Na <sub>2</sub> N <sub>2</sub> O <sub>3</sub> .	<b>Fig. S14</b>
15.	Emission spectra of DQ <sub>468</sub> to Cu <sup>+</sup>	<b>Fig. S15</b>
16.	Frontier molecular orbitals of DQ <sub>468</sub> in UV-vis absorption.	<b>Fig. S16</b>
17.	Frontier molecular orbitals of [Cu <sup>II</sup> (DQ <sub>468</sub> )Cl] <sup>+</sup> in UV-vis absorption.	<b>Fig. S17</b>
18.	Frontier molecular orbitals of [Cu <sup>I</sup> (DQ <sub>468</sub> )] <sup>+</sup> in UV-vis absorption.	<b>Fig. S18</b>

19.	Frontier molecular orbitals of $[\text{Cu}^{\text{I}}(\text{DQ}_{468})]^+$ in UV-vis absorption.	<b>Fig. S19</b>
20.	Frontier molecular orbitals of $[\text{Cu}^{\text{I}}(\text{DQ}_{468})]^+$ in UV-vis absorption.	<b>Fig. S20</b>
21.	UV-vis spectra of $[\text{Cu}^{\text{II}}(\text{DQ}_{468})\text{Cl}]$ towards HNO.	<b>Fig. S21</b>
22.	Some selected geometrical parameters (bond lengths and bond angles) of $\text{DQ}_{468}$ in ground state calculated at B3LYP/6-31G (d) Levels.	<b>Table S1</b>
23.	Some selected geometrical parameters (bond lengths and bond angles) for $[\text{Cu}^{\text{II}}(\text{DQ}_{468})\text{Cl}]^+$ in the ground state calculated at B3LYP/6-31G (d) Levels.	<b>Table S2</b>
24.	<b>Some selected geometrical parameters (bond lengths and bond angles) for <math>[\text{Cu}^{\text{I}}(\text{DQ}_{468})]^+</math> in the ground state calculated at B3LYP/6-31G (d) Levels.</b>	<b>Table S3</b>
25.	<b>Vertical excitation energies and oscillator strengths (<math>f_{\text{cal}}</math>) of some low-lying excited singlet states obtained from TDDFT// B3LYP/6-31G (d) calculations of <math>\text{DQ}_{468}</math></b>	<b>Table S4</b>
26.	<b>Vertical excitation energies and oscillator strengths (<math>f_{\text{cal}}</math>) of some low-lying excited singlet states obtained from TDDFT// B3LYP/6-31G(d) calculations of <math>[\text{Cu}^{\text{II}}(\text{DQ}_{468})\text{Cl}]^+</math></b>	<b>Table S5</b>
27.	<b>Vertical excitation energies and oscillator strengths (<math>f_{\text{cal}}</math>) of some low-lying excited singlet states obtained from TDDFT// B3LYP/6-31G (d) calculations of <math>[\text{Cu}^{\text{I}}(\text{DQ}_{468})]^+</math></b>	<b>Table S6</b>
28.	<b>Comparative table for detection limit of HNO probes.</b>	<b>Table S7</b>

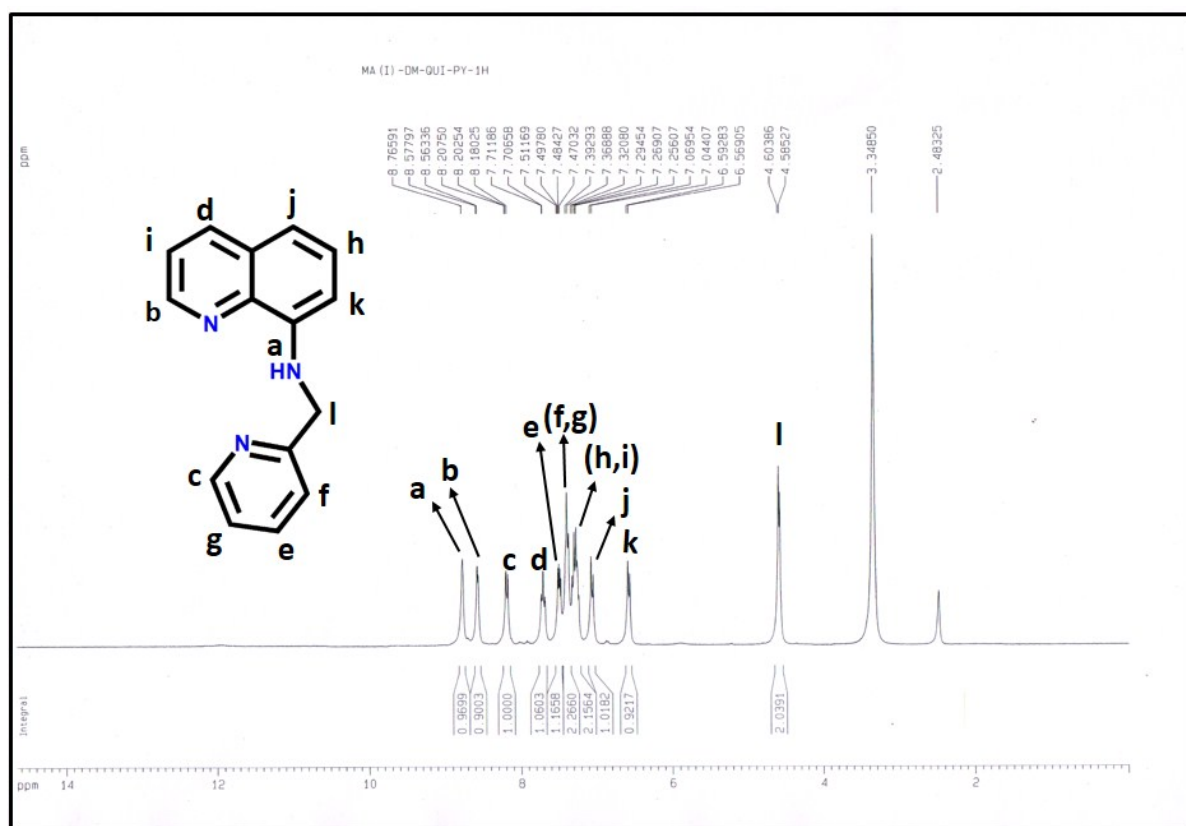


Fig.S1.  $^1\text{H}$  NMR spectrum of ( $\text{L}^1$ ) in  $\text{DMSO}-d_6$ .

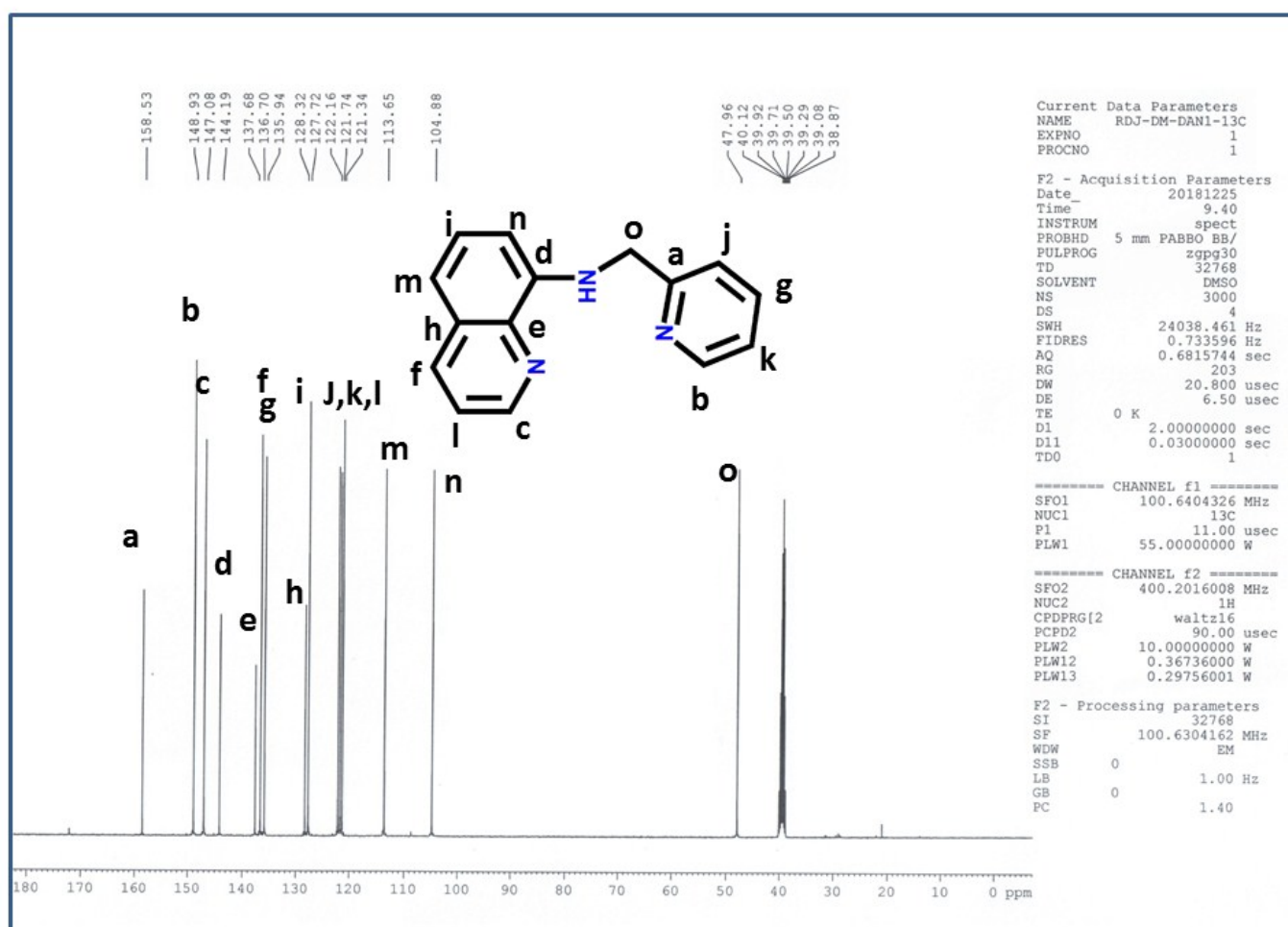
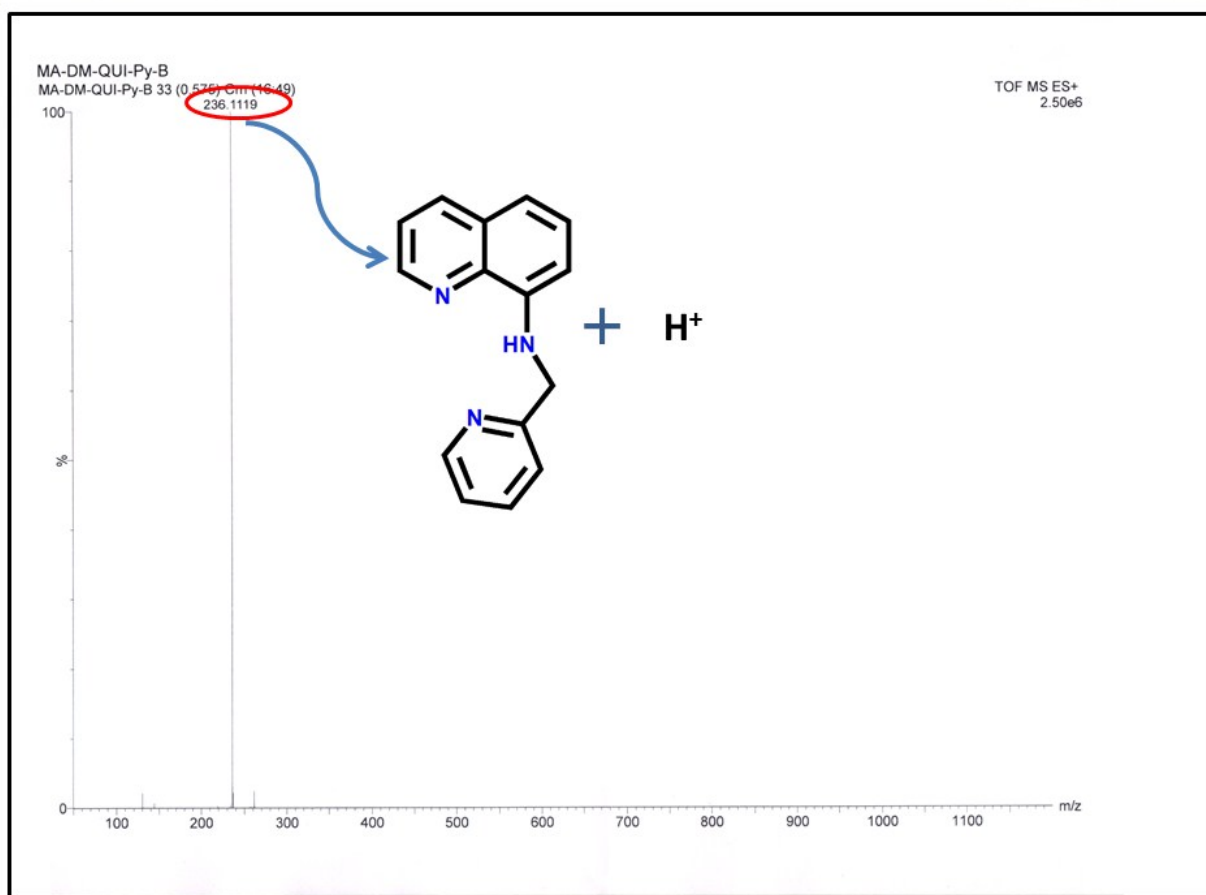


Fig. S2. <sup>13</sup>C NMR of (L<sup>1</sup>) in DMSO-*d*<sub>6</sub>.



**Fig. S3.** Mass spectrum of spectrum of (**L**<sup>1</sup>) in MeCN.

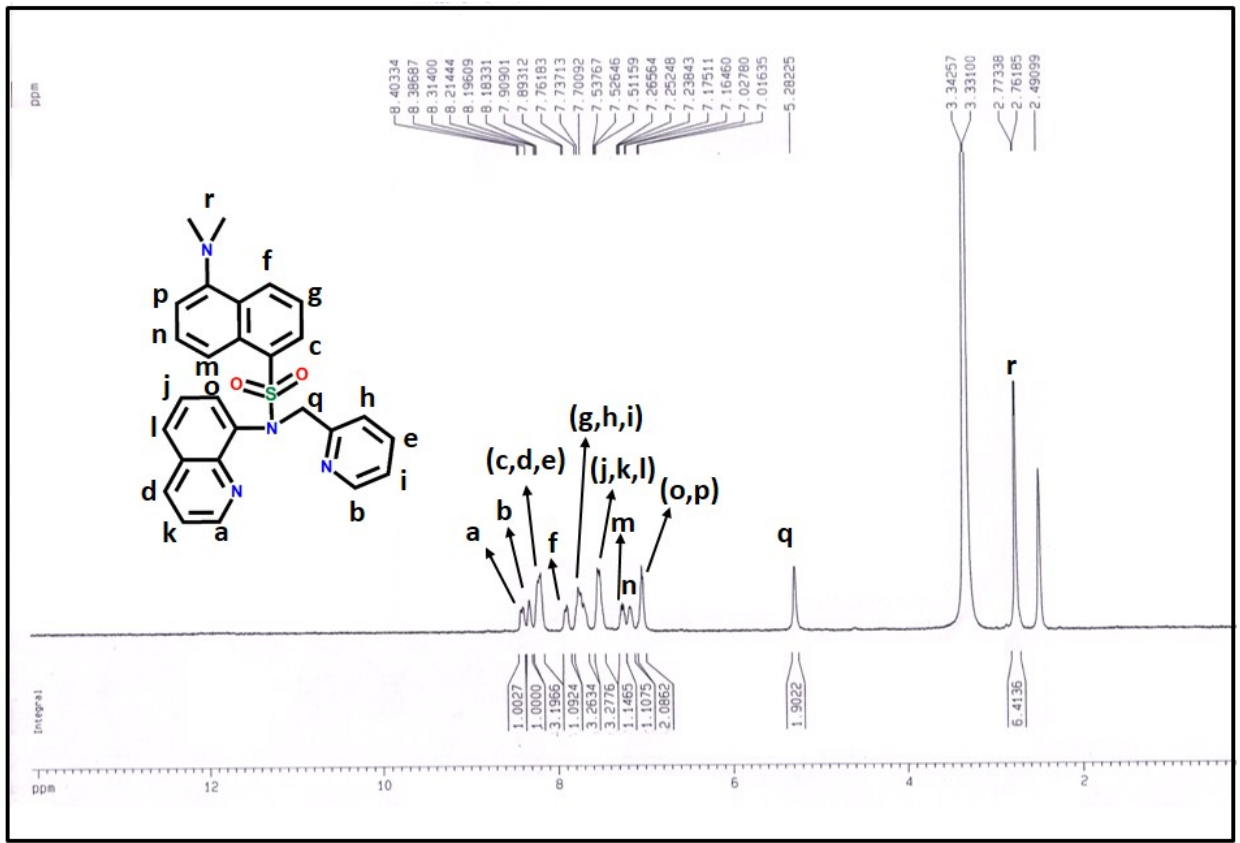


Fig.S4. <sup>1</sup>H NMR spectrum of DQ<sub>468</sub> in DMSO-*d*<sub>6</sub> (300Mz).

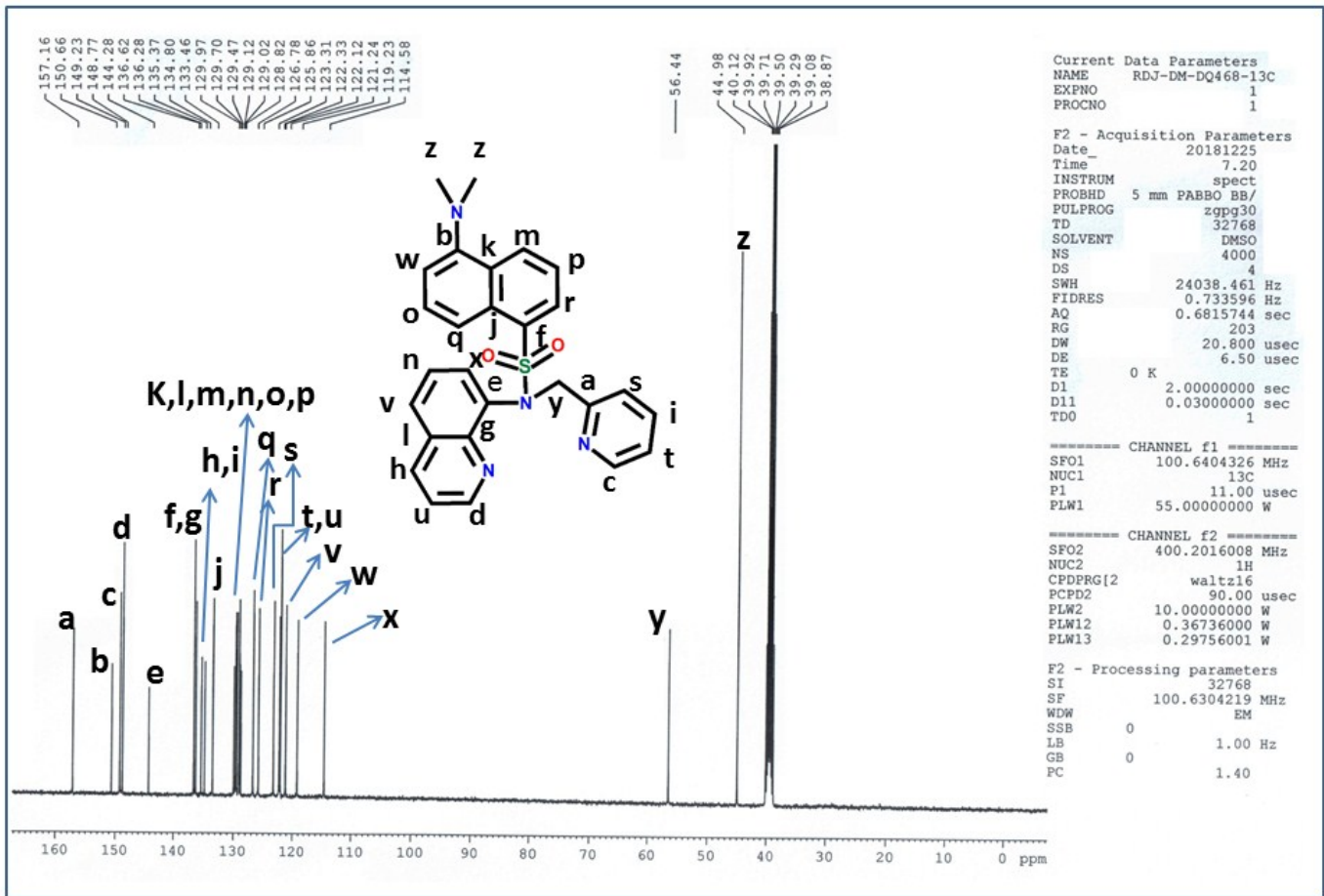


Fig. S5.  $^{13}\text{C}$  NMR of (DQ<sub>468</sub>) in DMSO-*d*<sub>6</sub>.

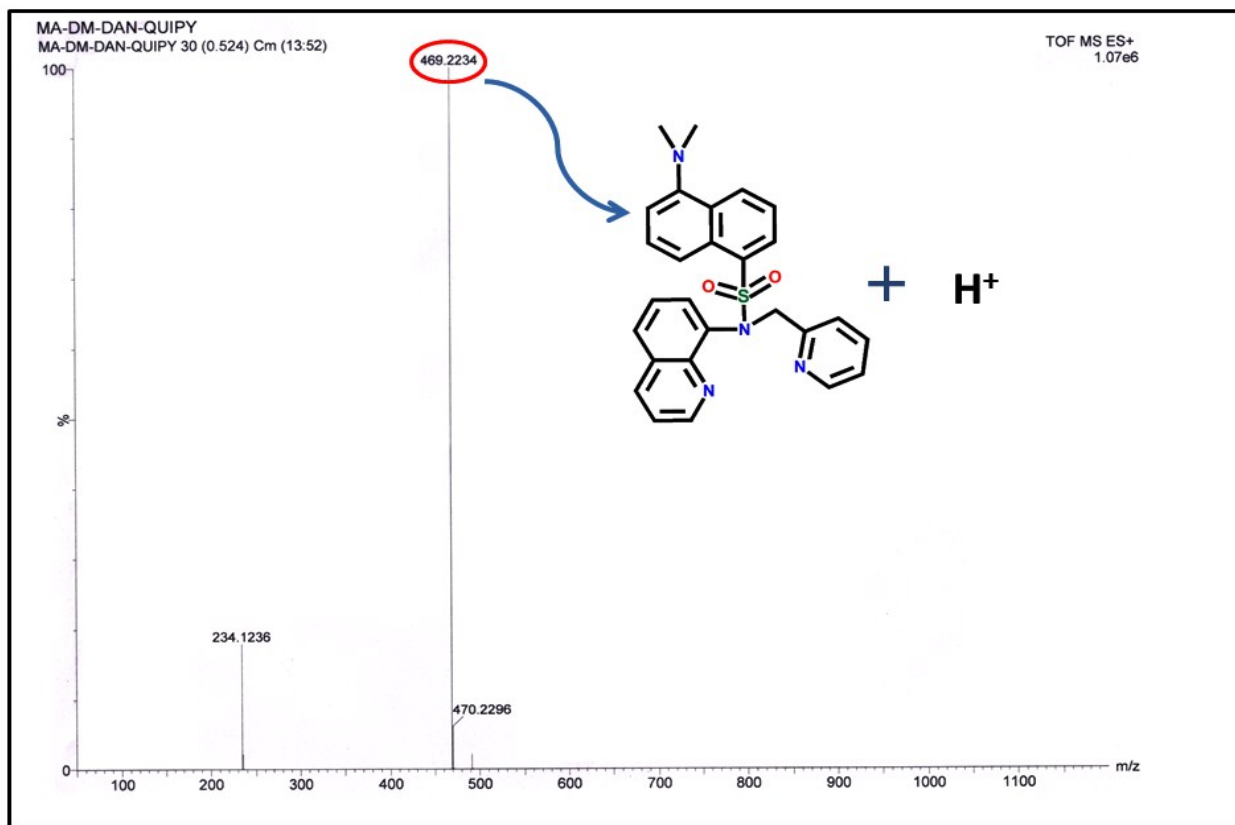


Fig. S6. Mass spectrum of **DQ<sub>468</sub>** in MeCN.



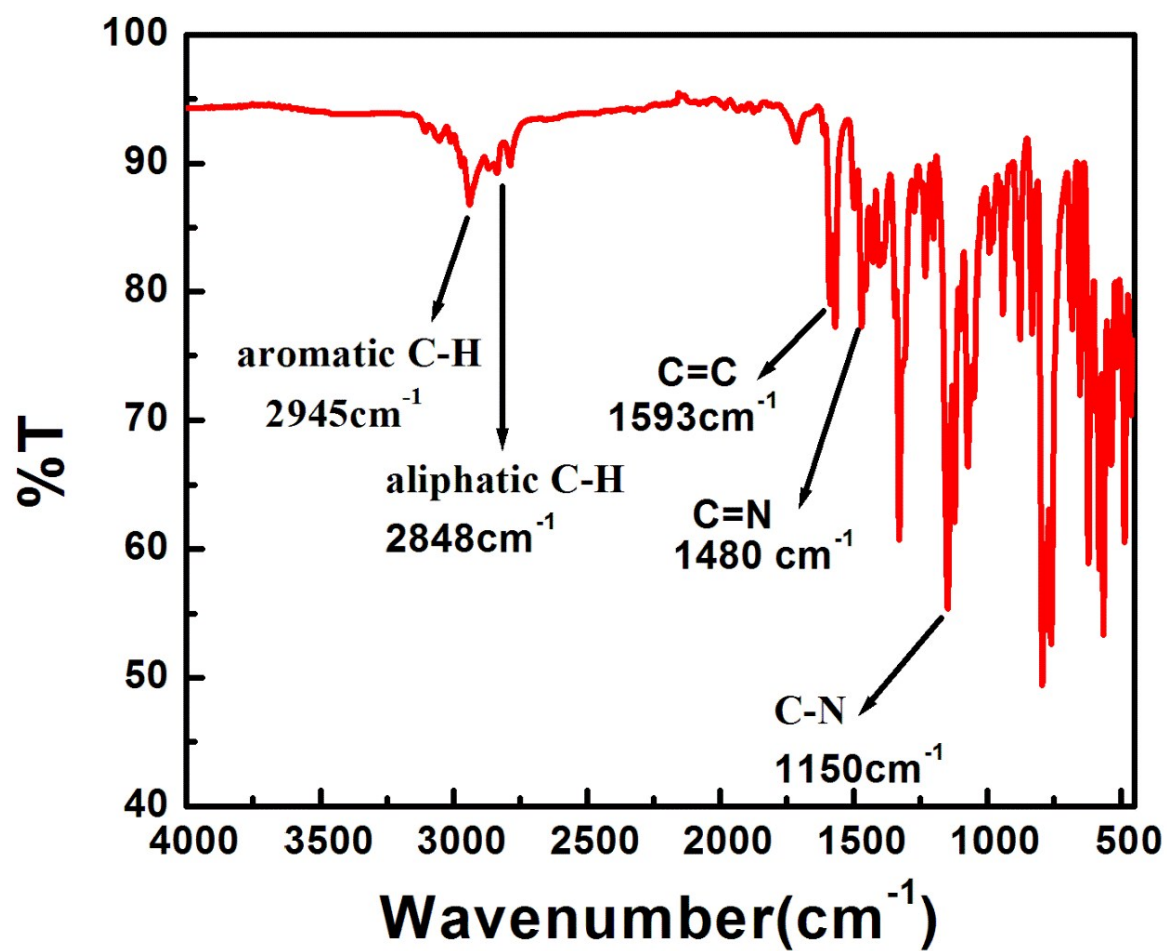


Fig. S7. Ir spectrum of DQ<sub>468</sub> .

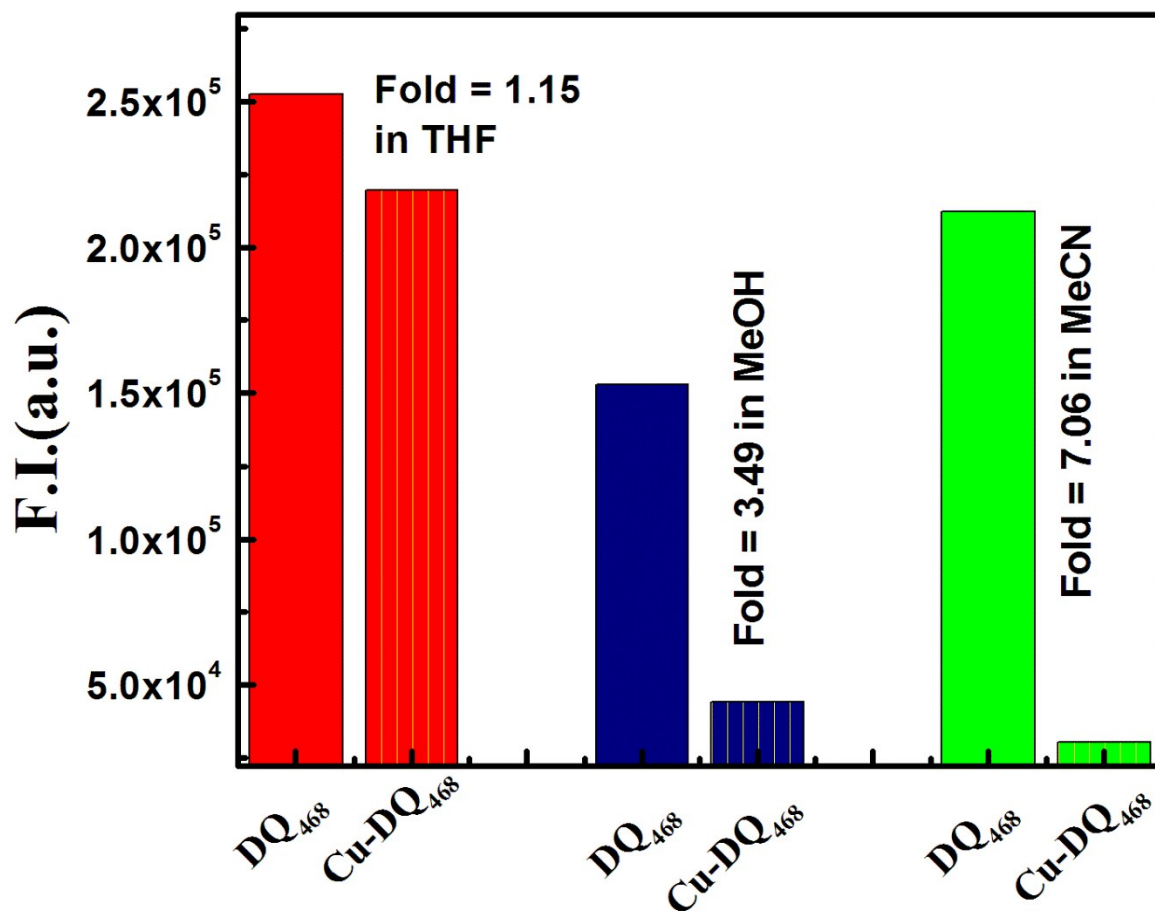


Fig. S8. Solvent selectivity of Cu(II)-complex formation.

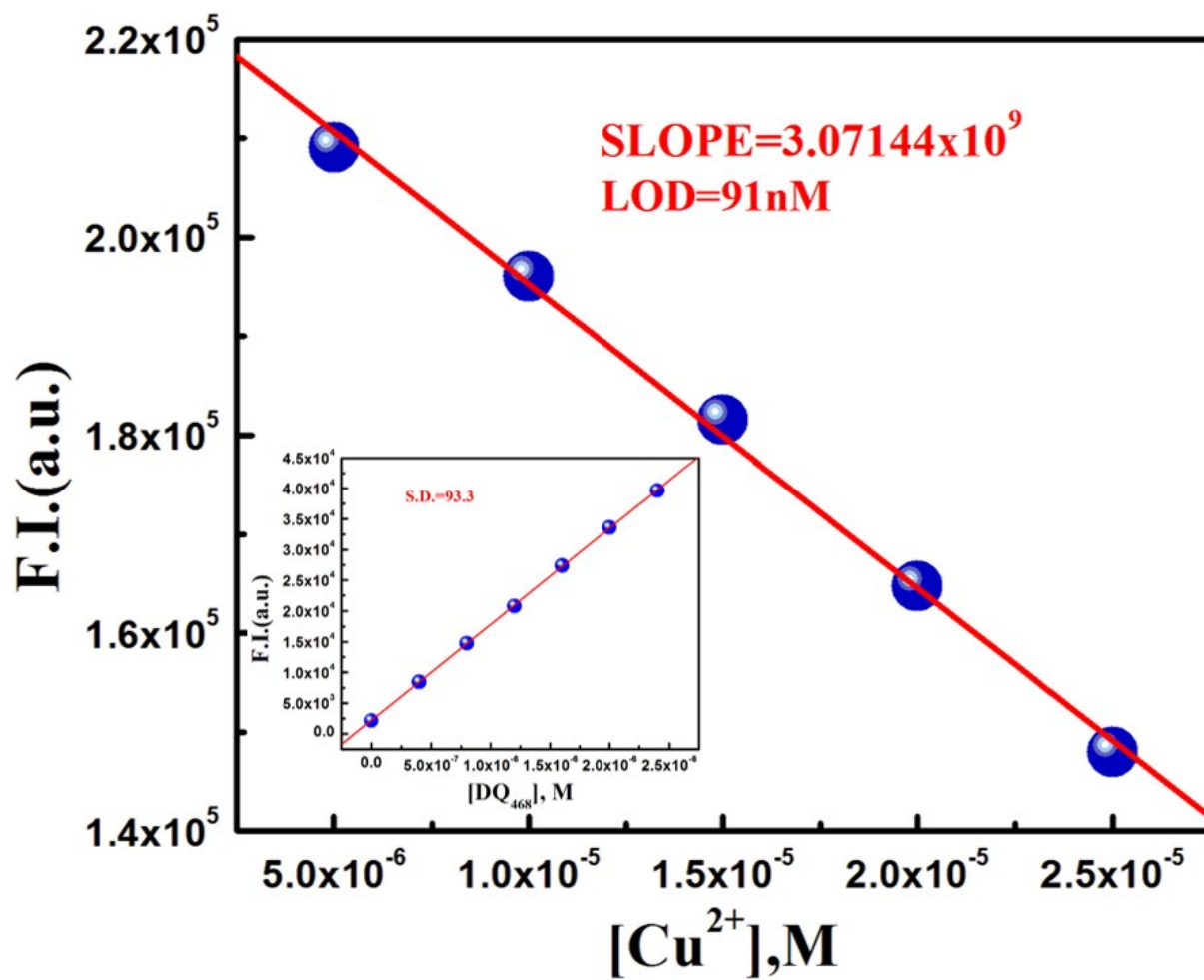


Fig. S9. LOD of  $\text{DQ}_{468}$  to  $\text{Cu}^{2+}$

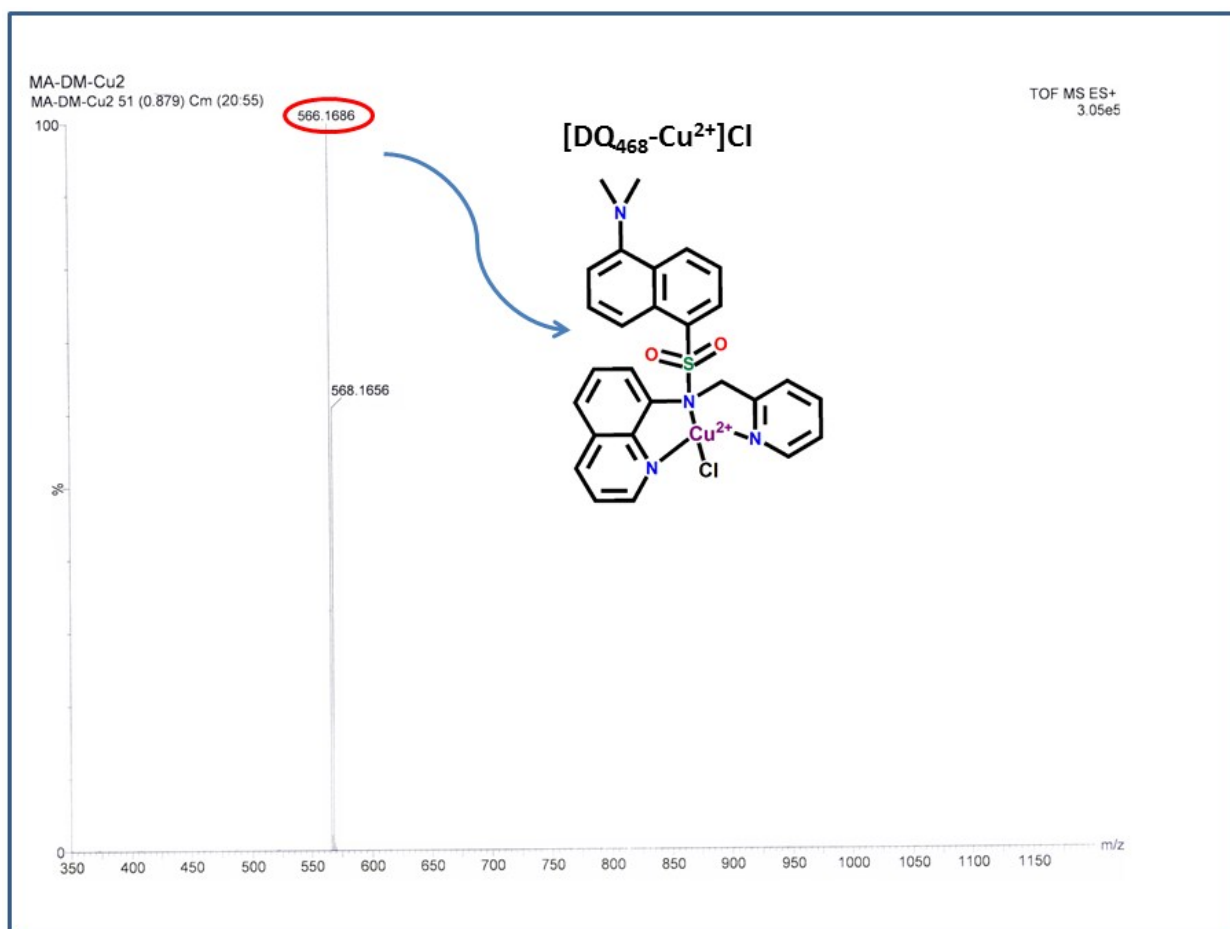


Fig. S10. Mass spectrum of [Cu<sup>II</sup>(DQ<sub>468</sub>)Cl].

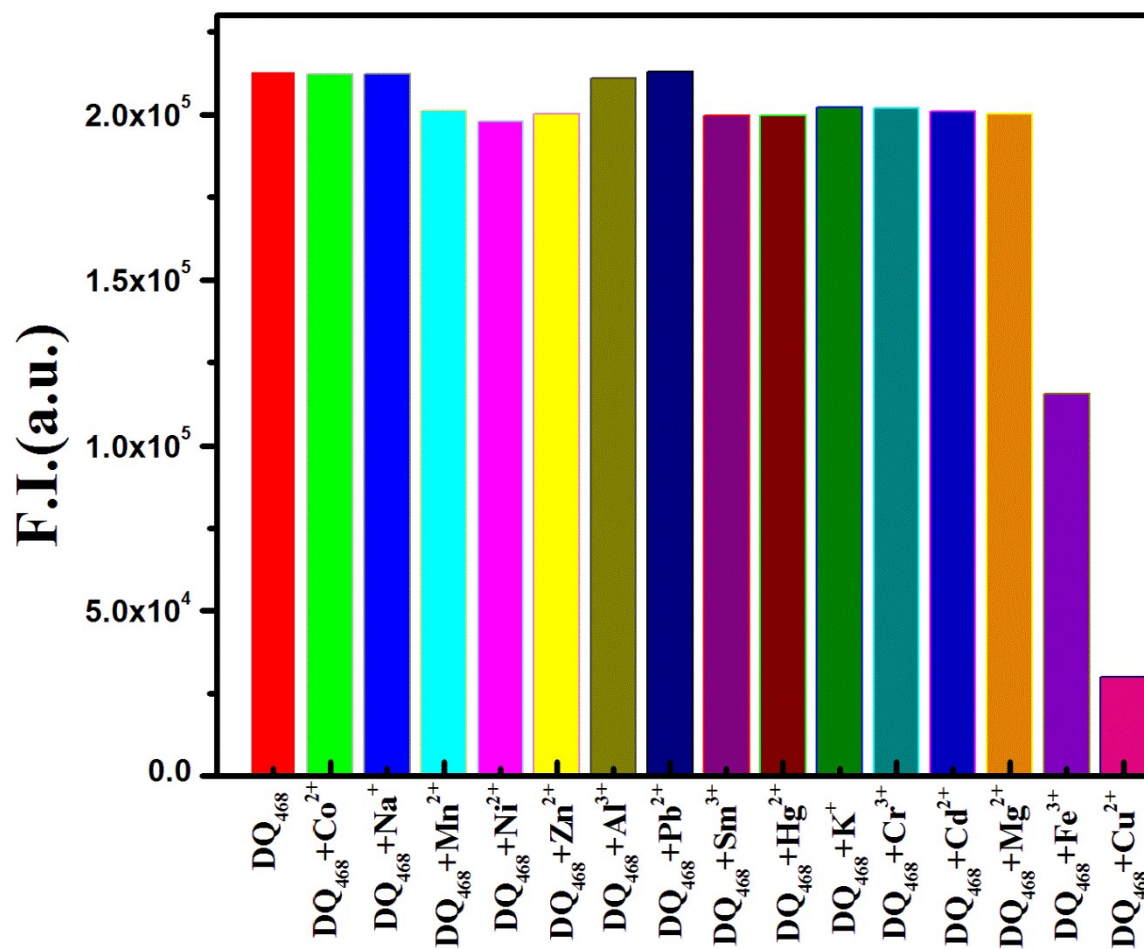


Fig. S11. Metal ion selectivity test of DQ<sub>468</sub>

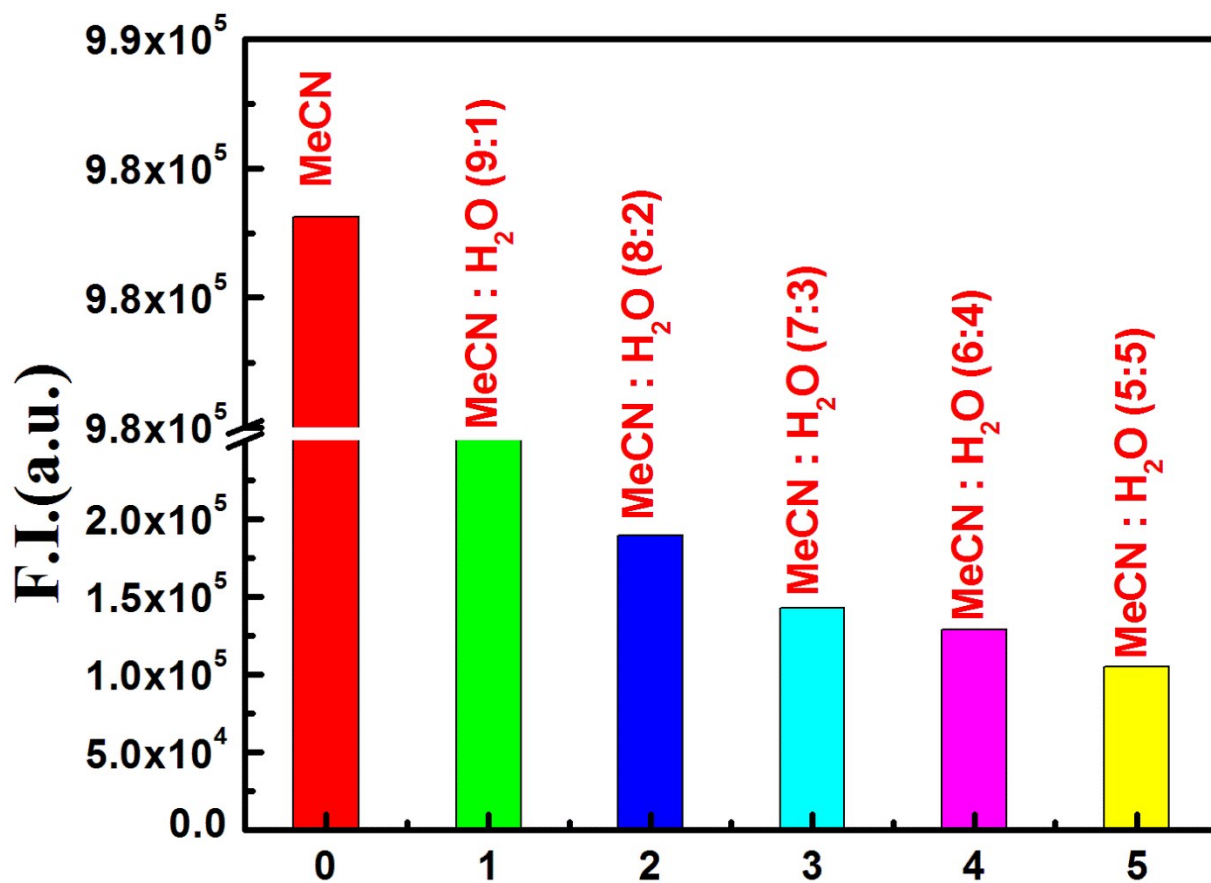


Fig. S12. Water variation on HNO induced reduction of Cu(II)-complex.

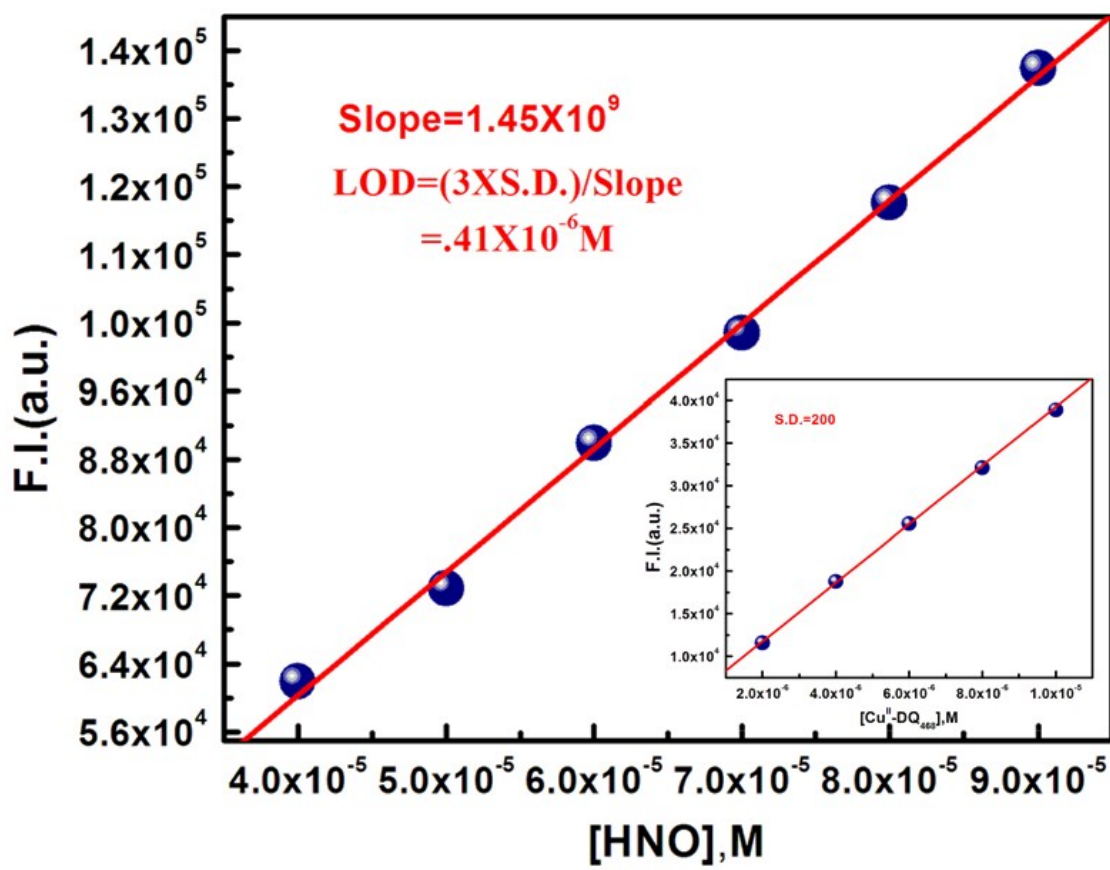


Fig. S13. LOD of Cu<sup>II</sup>-DQ<sub>468</sub> to HNO<sub>3</sub>.

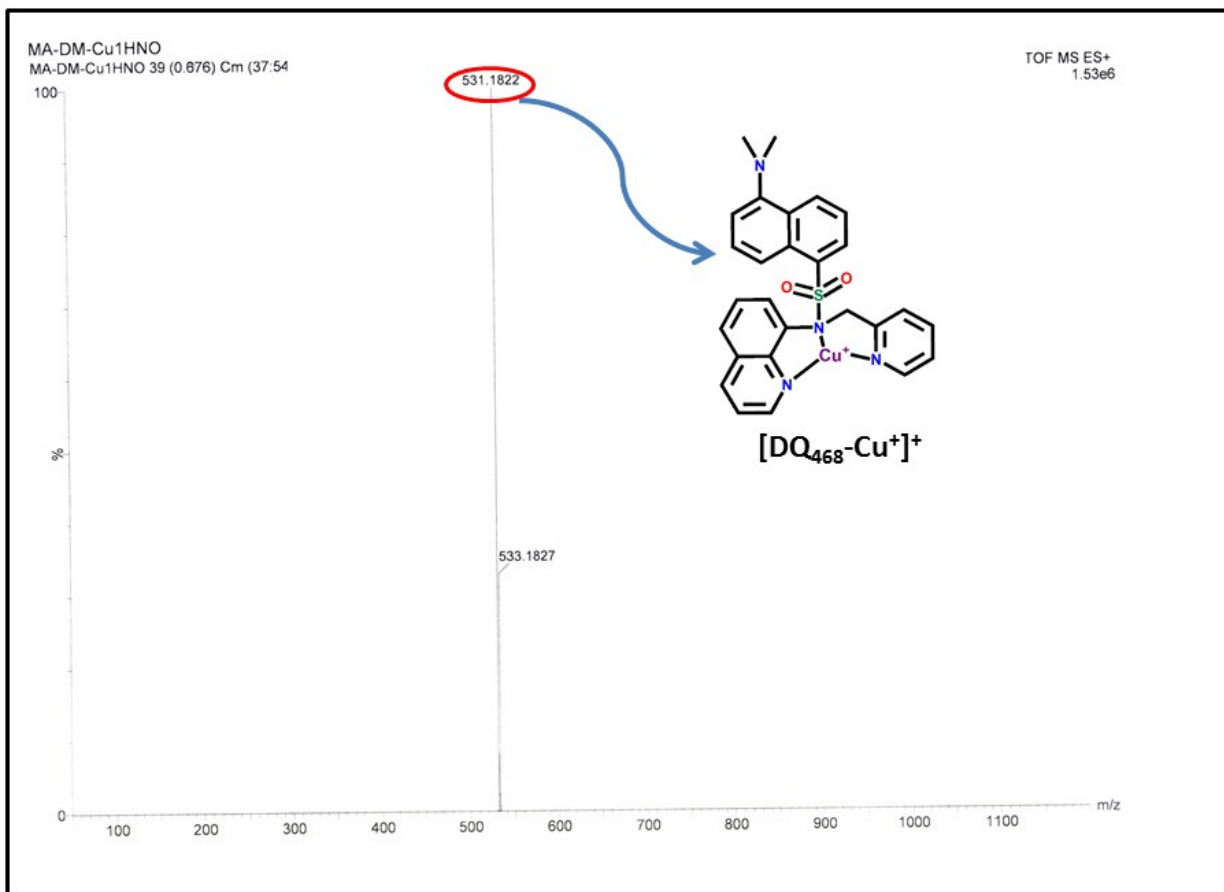


Fig. S14. Mass spectrum of [Cu(DQ<sub>468</sub>)Cl]<sup>+</sup> Na<sub>2</sub>N<sub>2</sub>O<sub>3</sub>.



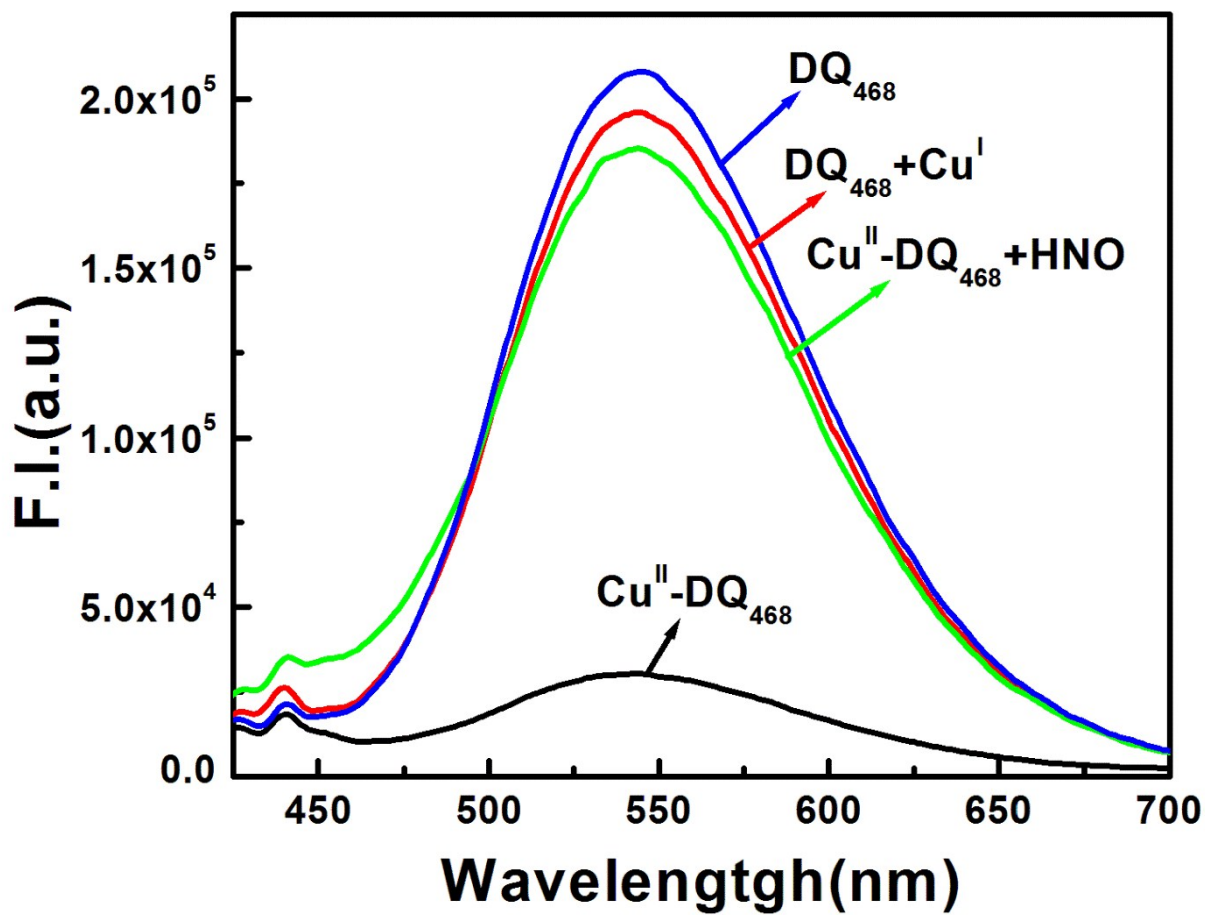


Fig. S15. Emission spectra of  $DQ_{468}$  in presence of  $Cu^+$ .

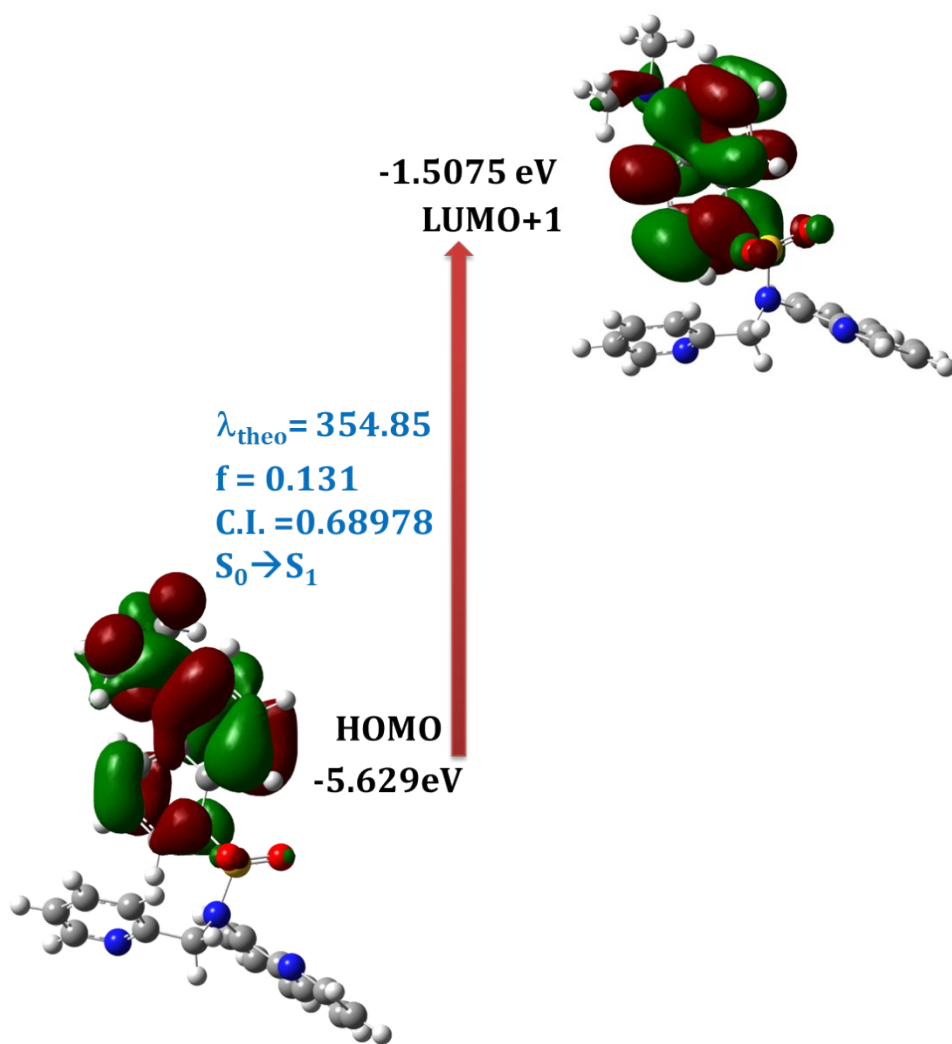
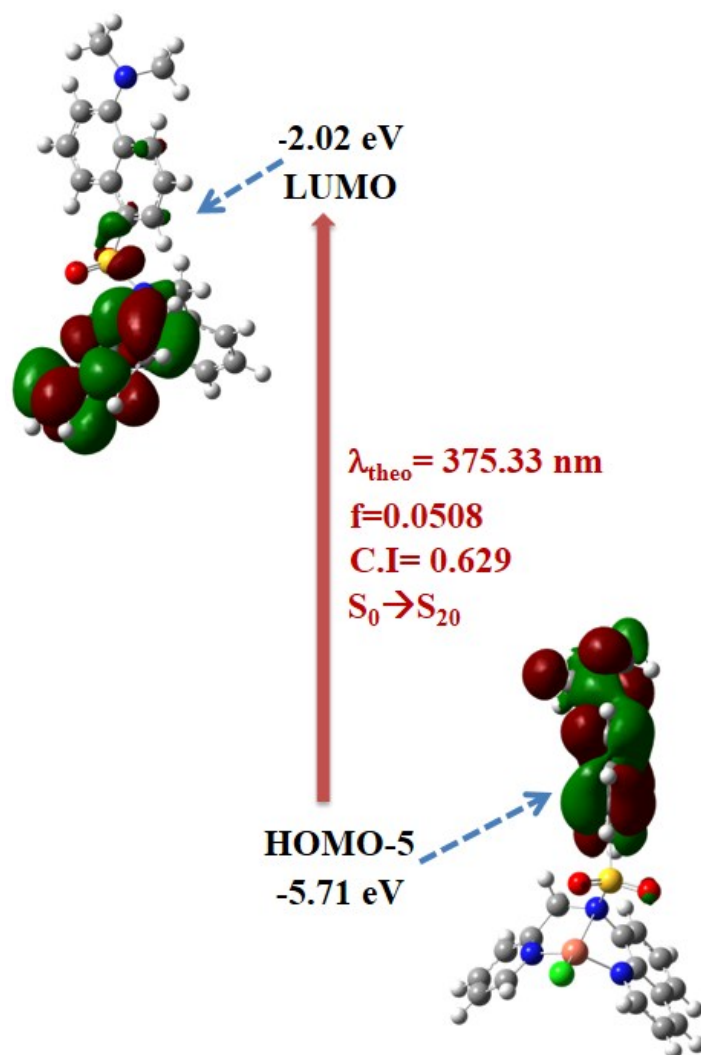
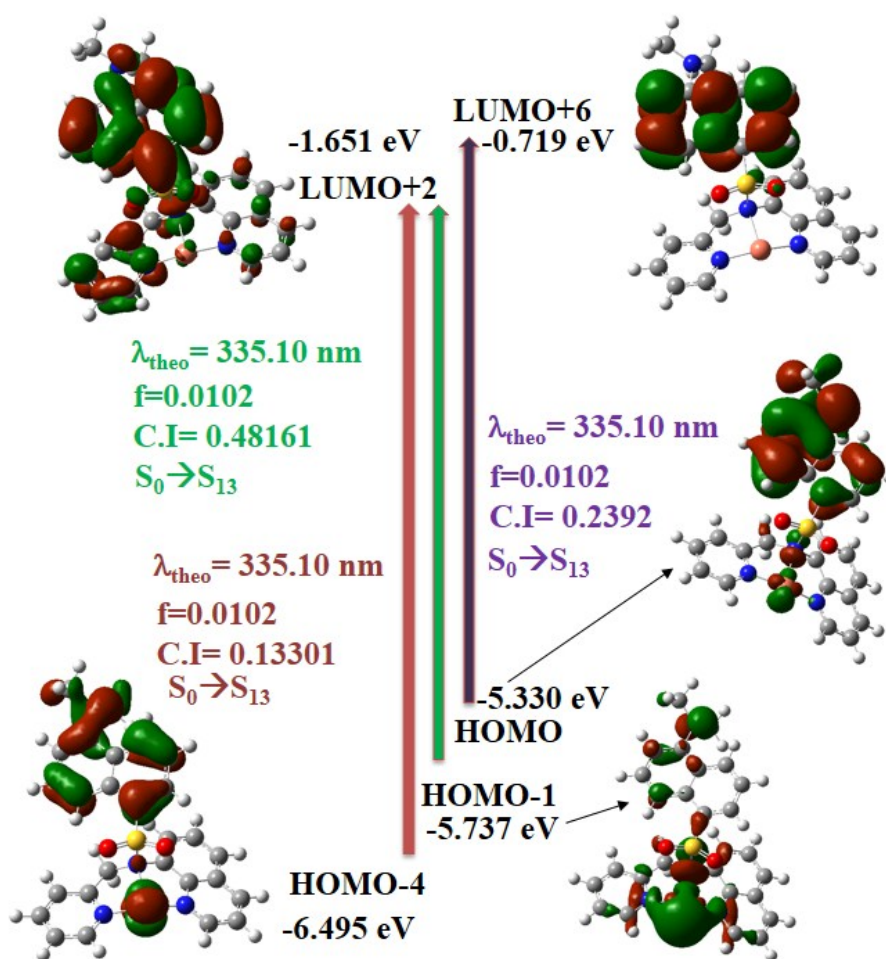


Fig.S16. Frontier molecular orbitals of **DQ<sub>468</sub>** in UV-vis absorption.



**Fig.S17.** Frontier molecular orbitals of  $[\text{Cu}^{\text{II}}(\text{DQ}_{468})\text{Cl}]^+$  in UV-vis absorption.



**Fig.S18.** Frontier molecular orbitals of  $[\text{Cu}'(\text{DQ}_{468})]^+$  in UV-vis absorption.

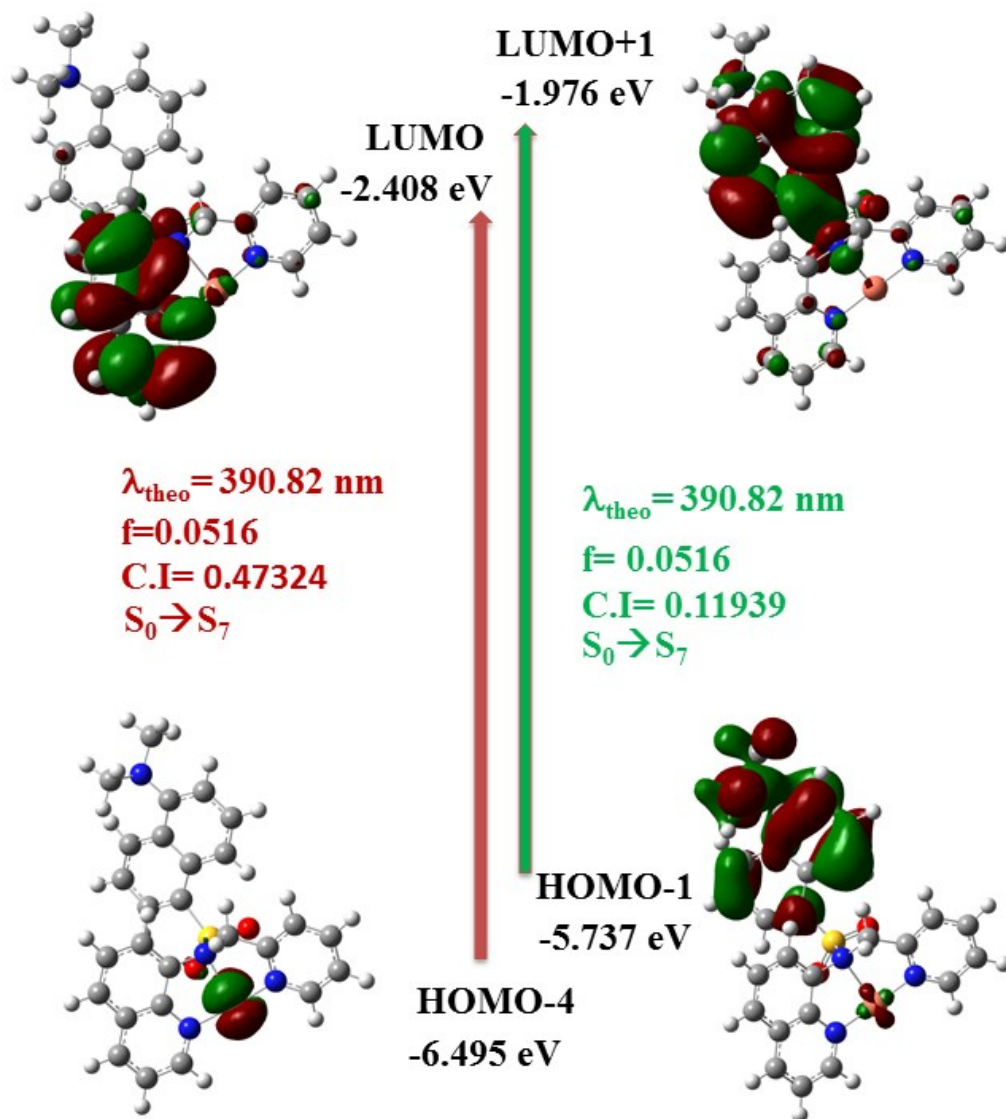


**Fig.S19.** Frontier molecular orbitals of  $[\text{Cu}'(\text{DQ}_{468})]^+$  in UV-vis absorption.

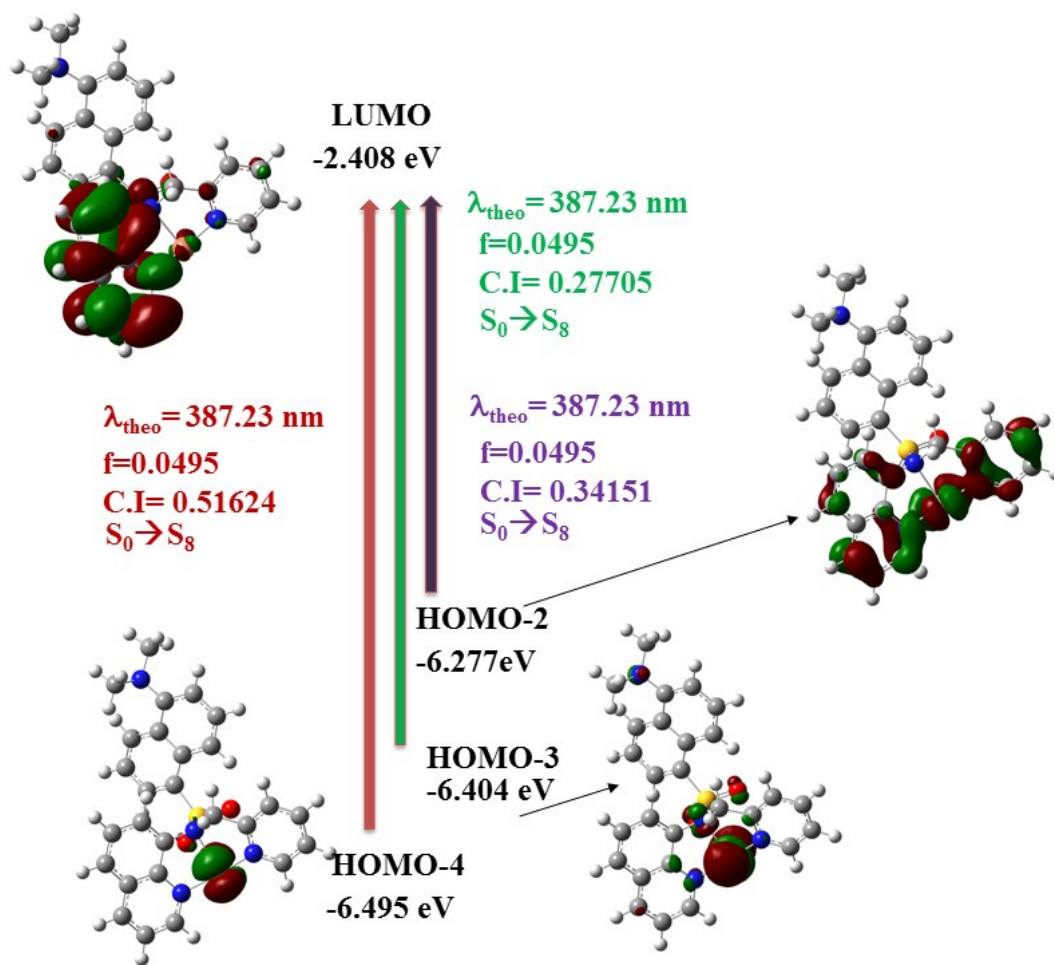


**Fig.S20.** Frontier molecular orbitals of  $[\text{Cu}'(\text{DQ}_{468})]^+$  in UV-vis absorption

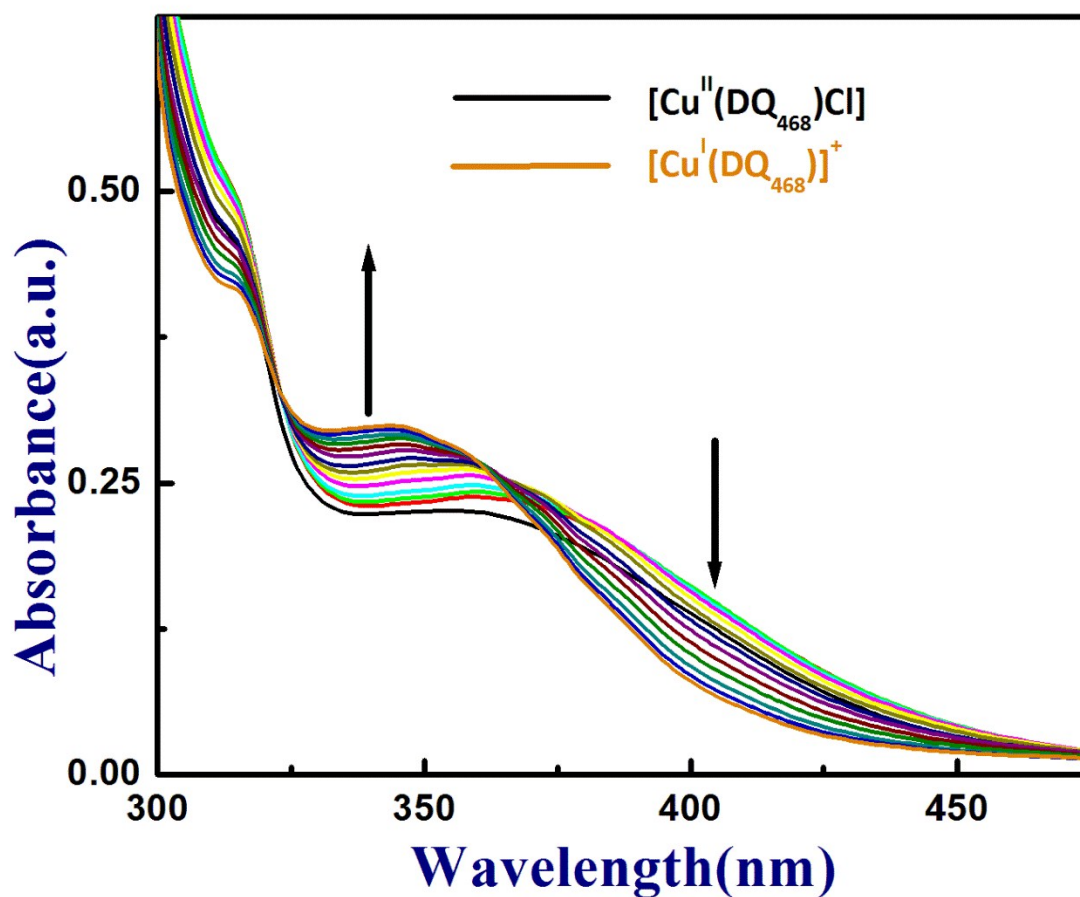


Fig. S21. UV-vis spectra of  $[\text{Cu}^{\text{II}}(\text{DQ}_{468})\text{Cl}]$  towards  $\text{HNO}_3$ .

**Table S1.** Some selected geometrical parameters (bond lengths and bond angles) of  $\text{DQ}_{468}$  in ground state calculated at B3LYP/6-31G (d) Levels.

Bond Lengths (Å)			
C6-S2	1.81	S2-N1	1.70
S2-O4	1.46	N1-C43	1.43
S2-O3	1.46	N1-C30	1.48
Bond Angles (°)			
C6-S2-N1	104.68	S2-N1-C43	116.03
O4-S2-O3	120.27	S2-N1-C30	116.48
N1-C43-C44	120.49	N1-C30-C33	113.16

**Table S2.** Some selected geometrical parameters (bond lengths and bond angles) for  $[\text{Cu}^{\text{II}}(\text{DQ}_{468})\text{Cl}]^+$  in the ground state calculated at B3LYP/6-31G (d) Levels.

Bond Lengths (Å)			
S2-C6	1.808	Cu33-N60	1.949
S2-N1	1.695	N1-Cu33	2.816
N1-C45	1.431	Cu33-Cl34	2.278
N1-C30	1.468	Cu33-N44	1.944
Bond Angles (°)			
S2-N1-C30	118.446	N60-Cu33-Cl34	112.665
S2-N1-C45	120.096	N44-Cu33-Cl34	114.493
N1-Cu33-N44	73.925		
N1-Cu33-N60	71.219		

**Table S3.** Some selected geometrical parameters (bond lengths and bond angles) for  $[\text{Cu}^{\text{I}}(\text{DQ}_{468})]^+$  in the ground state calculated at B3LYP/6-31G (d) Levels.

Bond Lengths (Å)			
C6-S2	1.7928	N43-Cu33	1.8746
S2-O4	1.4629	N1-Cu33	2.1991
S2-O3	1.4629	N59-Cu33	1.8749
S2-N1	1.7599		
Bond Angles (°)			
C6-S2-N1	108.5100	N1-Cu33-N59	86.7645
S2-N1-Cu33	98.1251	N43-Cu33-N59	156.9166
N1-Cu33-N43	87.3255		



**Table S4a.** Vertical excitation energy and oscillator strength ( $f_{\text{cal}}$ ) of low-lying excited singlet states obtained from TDDFT// B3LYP/6-31G(d) calculations of **DQ<sub>468</sub>** which is matched with the experimental one.

Electronic transition	Composition	Excitation energy	Oscillator strength ( $f_{\text{cal}}$ )	CI	$\lambda_{\text{exp}}$ (nm)
$S_0 \rightarrow S_1$	HOMO $\rightarrow$ LUMO+1 (123 $\rightarrow$ 125)	3.494 eV (354.85nm)	0.1310	0.68978	337

**Table S4b.** All vertical excitation energies and oscillator strengths ( $f_{\text{cal}}$ ) of some low-lying excited singlet states obtained from TDDFT// B3LYP/6-31G(d) calculations of **DQ<sub>468</sub>**.

Electronic transition	Composition	Excitation energy	Oscillator strength ( $f_{\text{cal}}$ )	CI	$\lambda_{\text{theo}}$ (nm)
$S_0 \rightarrow S_2$	<b>123 <math>\rightarrow</math> 124</b>	<b>3.5588 eV</b>	<b>0.0009</b>	<b>0.69982</b>	<b>348.38</b>
$S_0 \rightarrow S_3$	<b>122 <math>\rightarrow</math> 124</b>	<b>4.1961 eV</b>	<b>0.1322</b>	<b>0.62435</b>	<b>295.48</b>
	<b>123 <math>\rightarrow</math> 128</b>			<b>0.14947</b>	
$S_0 \rightarrow S_4$	<b>123 <math>\rightarrow</math> 126</b>	<b>4.2099 eV</b>	<b>0.0162</b>	<b>0.17684</b>	<b>294.51</b>
	<b>123 <math>\rightarrow</math> 128</b>			<b>0.48177</b>	
$S_0 \rightarrow S_5$	<b>123 <math>\rightarrow</math> 126</b>	<b>4.3426 eV</b>	<b>0.0002</b>	<b>0.67979</b>	<b>285.51</b>
$S_0 \rightarrow S_6$	<b>116 <math>\rightarrow</math> 124</b>	<b>4.3549 eV</b>	<b>0.0189</b>	<b>0.51975</b>	<b>284.70</b>
	<b>117 <math>\rightarrow</math> 124</b>			<b>0.15908</b>	
	<b>118 <math>\rightarrow</math> 124</b>			<b>0.36919</b>	
	<b>122 <math>\rightarrow</math> 124</b>			<b>0.18026</b>	
$S_0 \rightarrow S_7$	<b>122 <math>\rightarrow</math> 125</b>	<b>4.4352 eV</b>	<b>0.0010</b>	<b>0.68757</b>	<b>279.55</b>
$S_0 \rightarrow S_8$	<b>117 <math>\rightarrow</math> 124</b>	<b>4.5105 eV</b>	<b>0.0352</b>	<b>0.10643</b>	<b>274.88</b>
	<b>119 <math>\rightarrow</math> 124</b>			<b>0.50113</b>	
$S_0 \rightarrow S_9$	<b>121 <math>\rightarrow</math> 124</b>	<b>4.5430 eV</b>	<b>0.0066</b>	<b>0.6754</b>	<b>272.91</b>
$S_0 \rightarrow S_{10}$	<b>121 <math>\rightarrow</math> 125</b>	<b>4.5719 eV</b>	<b>0.0394</b>	<b>0.66793</b>	<b>271.19</b>

**Table S5a.** Vertical excitation energy and oscillator strength ( $f_{\text{cal}}$ ) of low-lying excited singlets obtained from TDDFT// B3LYP/6-31G (d) calculations of  $[\text{Cu}^{\text{II}}(\text{DQ}_{468})\text{Cl}]^+$  complex which is matched with the experimental one.

Electronic Transition	Composition	Excitation energy	Oscillator strength ( $f_{\text{cal}}$ )	CI	$\lambda_{\text{exp}}$ (nm)
$S_0 \rightarrow S_{20}$	HOMO-5 $\rightarrow$ LUMO (141 $\rightarrow$ 147)	3.3033 eV (375.33nm)	0.0508	0.629	370

**Table S5b.** All vertical excitation energies and oscillator strengths ( $f_{\text{cal}}$ ) of some low-lying excited singlets obtained from TDDFT// B3LYP/6-31G (d) calculations of  $[\text{Cu}^{\text{II}}(\text{DQ}_{468})\text{Cl}]^+$  complex.

Electronic transition	Composition	Excitation energy	Oscillator strength ( $f_{\text{cal}}$ )	CI	$\lambda_{\text{theo}}$ (nm)
$S_0 \rightarrow S_{10}$	144 $\rightarrow$ 149	2.7669 eV	0.0013	0.661	448.10
$S_0 \rightarrow S_{11}$	144 $\rightarrow$ 148	2.8810 eV	0.0021	0.667	430.36
	144 $\rightarrow$ 149			0.212	
$S_0 \rightarrow S_{12}$	146 $\rightarrow$ 150	2.9085 eV	0.0030	0.680	426.28
	146 $\rightarrow$ 151			0.114	
$S_0 \rightarrow S_{13}$	142 $\rightarrow$ 149	2.9834 eV	0.0039	0.468	415.59
	143 $\rightarrow$ 148			0.213	
$S_0 \rightarrow S_{14}$	142 $\rightarrow$ 149	3.0358 eV	0.0029	0.128	408.40
	143 $\rightarrow$ 148			0.100	
	145 $\rightarrow$ 150			0.603	
	145 $\rightarrow$ 151			0.110	
$S_0 \rightarrow S_{15}$	143 $\rightarrow$ 148	3.0578 eV	0.0049	0.13245	405.47
	145 $\rightarrow$ 150			0.29261	
	146 $\rightarrow$ 151			0.29932	
	146 $\rightarrow$ 152			0.52448	
$S_0 \rightarrow S_{16}$	143 $\rightarrow$ 148	3.0652 eV	0.0030	0.62561	404.49
$S_0 \rightarrow S_{17}$	142 $\rightarrow$ 148	3.1582 eV	0.0003	0.68404	392.58
	142 $\rightarrow$ 149			0.13745	
$S_0 \rightarrow S_{18}$	145 $\rightarrow$ 151	3.1867 eV	0.0013	0.34507	389.07
	145 $\rightarrow$ 152			0.59806	
$S_0 \rightarrow S_{19}$	142 $\rightarrow$ 149	3.2509 eV	0.0042	0.32038	381.39
	143 $\rightarrow$ 147			0.10125	
	143 $\rightarrow$ 148			0.14708	
	143 $\rightarrow$ 149			0.37583	
$S_0 \rightarrow S_{20}$	141 $\rightarrow$ 147	3.3033 eV	0.0508	0.62904	375.33

**Table S6a.** Vertical excitation energy and oscillator strength ( $f_{cal}$ ) of low-lying excited singlets obtained from TDDFT// B3LYP/6-31G (d) calculations of  $[Cu'(DQ_{468})]^+$  complex which is matched with the experimental one.

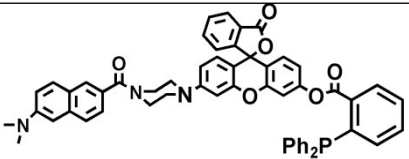
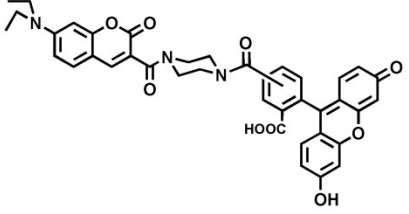
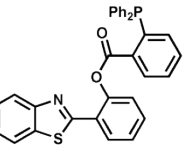
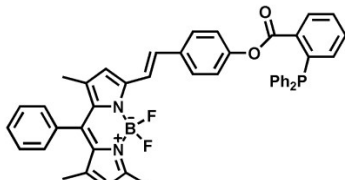
Electronic transition	Composition	Excitation energy	Oscillator strength ( $f_{cal}$ )	CI	$\lambda_{exp}$ (nm)
$S_0 \rightarrow S_{13}$	HOMO-4 $\rightarrow$ LUMO+2 (133 $\rightarrow$ 140)	3.699 eV (335.10nm)	0.0102	0.13301	340
	HOMO-1 $\rightarrow$ LUMO+2 (136 $\rightarrow$ 140)			0.48161	
	HOMO $\rightarrow$ LUMO+6 (137 $\rightarrow$ 144)			0.23920	
$S_0 \rightarrow S_7$	HOMO-4 $\rightarrow$ LUMO (133 $\rightarrow$ 138)	3.1724 eV (390.82 nm)	0.0516	0.47324	
	HOMO-1 $\rightarrow$ LUMO+1 (136 $\rightarrow$ 139)			0.11939	
$S_0 \rightarrow S_8$	HOMO-4 $\rightarrow$ LUMO (133 $\rightarrow$ 138)	3.2018 eV (387.23nm)	0.0495	0.51624	
	HOMO-3 $\rightarrow$ LUMO (134 $\rightarrow$ 138)			0.27705	
	HOMO-2 $\rightarrow$ LUMO (135 $\rightarrow$ 138)			0.34151	

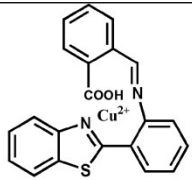
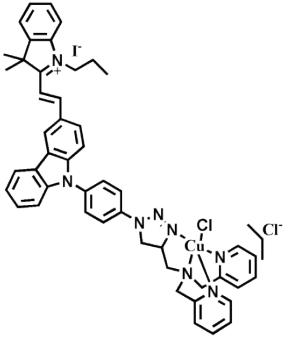
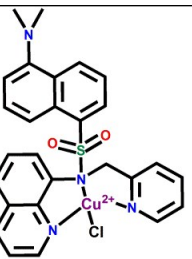
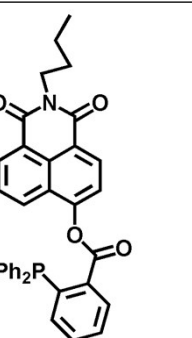
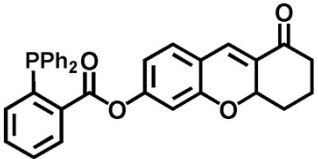
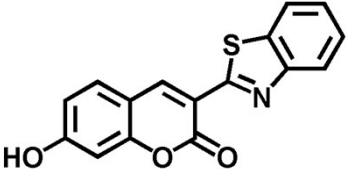
**Table S6b.** All vertical excitation energies and oscillator strengths ( $f_{cal}$ ) of some low-lying excited singlets obtained from TDDFT// B3LYP/6-31G(d) calculations of  $[Cu'(DQ_{468})]^+$  complex .

Electronic transition	Composition	Excitation energy	Oscillator strength ( $f_{cal}$ )	CI	$\lambda_{theo}$ (nm)
$S_0 \rightarrow S_7$	133 $\rightarrow$ 138	3.1724 eV	0.0516	0.47324	390.82
	136 $\rightarrow$ 139			0.11939	
$S_0 \rightarrow S_8$	133 $\rightarrow$ 138	3.2018 eV	0.0495	0.51624	387.23
	134 $\rightarrow$ 138			0.27705	
	135 $\rightarrow$ 138			0.34151	
$S_0 \rightarrow S_9$	137 $\rightarrow$ 141	3.3675 eV	0.0002	0.67789	368.18
$S_0 \rightarrow S_{10}$	132 $\rightarrow$ 138	3.3891 eV	0.0005	0.67855	365.83
	137 $\rightarrow$ 141			0.16656	
$S_0 \rightarrow S_{11}$	137 $\rightarrow$ 142	3.5407 eV	0.0015	0.69295	350.17
	137 $\rightarrow$ 143			0.10158	
$S_0 \rightarrow S_{12}$	134 $\rightarrow$ 139	3.6471 eV	0.0032	0.14748	339.95
	134 $\rightarrow$ 140			0.37982	
	135 $\rightarrow$ 139			0.17712	
	135 $\rightarrow$ 140			0.24647	

	136 ->140			0.44043	
$S_0 \rightarrow S_{13}$	133->140	3.6999 eV	0.0102	0.13301	335.10
	136 ->140			0.48161	
	137 ->144			0.23920	
$S_0 \rightarrow S_{14}$	135 ->139	3.7298 eV	0.0015	0.37668	332.42
	135 ->140			0.14490	
	137 ->143			0.11738	
	137 ->144			0.52594	
$S_0 \rightarrow S_{15}$	134 ->139	3.7414 eV	0.0080	0.23671	331.39
	134 ->140			0.44980	
	137 ->144			0.28323	
$S_0 \rightarrow S_{16}$	133 ->139	3.7803 eV	0.0019	0.26571	327.98
	133 ->140			0.60691	
	135 ->139			0.19626	

**Table S7:** Comparative table for detection limit of HNO probes.

HNO Probes	$\lambda_{em}$	LOD ( $\mu M$ )	REFERENCES
	541nm	0.59	1
	517nm	1.4	2
	460nm	0.98	3
	586nm	2	4

	450nm	9	5
	595nm	23	6
	543nm	0.4	THIS WORK
	546nm	0.5	7
	512nm	0.59	8
	490nm	0.64	9

#### References:

1. X. Zhu, M. Xiong, HW Liu, GJ Mao, L Zhou, J. Zhang, X. Hu, XB Zhang and Weihong Tan, *Chem. Commun.*, 2016, **52**, 733.
2. H. Zhang, R. Liu, Y. Tan, W H. Xie, H. Lei, HY. Cheung and H. Sun, *ACS Appl. Mater. Interfaces*, 2015, **7**, 5438

3. HM. Lv, Y. Chen, J. Lei, CTong Aua and Shuang-Feng Yin *Anal. Methods*, 2015, **7**, 3883
4. F. Ali, S. Sreedharan, AH. Ashoka, H K. Saeed, CGW. Smythe, J A. Thomas, and A. Das, *Anal. Chem.* 2017, **89**, 12087.
5. S. Palanisamy, YL. Wang, YJ. Chen, CY. Chen, FT. Tsai, WF. Liaw and YM. Wang, *Molecules*, 2018, **23**, 2551.
6. HJ. Lv, RF. Ma, XT. Zhang, MH. Li , YT. Wang , S. Wang, GW. Xing, *Tetrahedron*, 2016, **72** , 5495.
7. C. Liu, H. Wu, Z. Wang, C. Shao, B. Zhu and X. Zhang, *Chem. Commun.*, 2014, **50**, 6013.
8. K. Zheng, W. Lin, D. Cheng, H. Chen, Y. Liub and K. Liu, *Chem. Commun.*, 2015, **51**, 5754.
9. B. Dong , K. Zheng , Y. Tang and W. Lin, *J. Mater. Chem. B*, 2016, **4**, 1263.